cis-acting RNA elements required for replication of bovine viral diarrhea virus-hepatitis C virus 5' nontranslated region chimeras

I. Frolov, M. S. McBride and C. M. Rice

RNA 1998 4: 1418-1435

RNA (1998), *4*:1418–1435. Cambridge University Press. Printed in the USA.

cis-acting RNA elements required for replication of bovine viral diarrhea virus–hepatitis C virus 5′ nontranslated region chimeras

ILYA FROLOV,[1] M. SCOTT McBRIDE,[1,2] and CHARLES M. RICE[1]

Department of Molecular Microbiology, Washington University School of Medicine, St. Louis, Missouri 63110-1093, USA

ABSTRACT

Pestiviruses, such as bovine viral diarrhea virus (BVDV), share many similarities with hepatitis C virus (HCV) yet are more amenable to virologic and genetic analysis. For both BVDV and HCV, translation is initiated via an internal ribosome entry site (IRES). Besides IRES function, the viral 5′ nontranslated regions (NTRs) may also contain *cis*-acting RNA elements important for viral replication. A series of chimeric RNAs were used to examine the function of the BVDV 5′ NTR. Our results show that: (1) the HCV and the encephalomyocarditis virus (EMCV) IRES element can functionally replace that of BVDV; (2) two 5′ terminal hairpins in BVDV genomic RNA are important for efficient replication; (3) replacement of the entire BVDV 5′ NTR with those of HCV or EMCV leads to severely impaired replication; (4) such replacement chimeras are unstable and efficiently replicating pseudorevertants arise; (5) pseudorevertant mutations involve deletion of 5′ sequences and/or acquisition of novel 5′ sequences such that the 5′ terminal 3–4 bases of BVDV genome RNA are restored. Besides providing new insight into functional elements in the BVDV 5′ NTR, these chimeras may prove useful as pestivirus vaccines and for screening and evaluation of anti-HCV IRES antivirals.

Keywords: antiviral screening; hepatitis C virus; pestivirus; RNA replication; translation initiation

INTRODUCTION

The *Flavivirdae* is an important family of human and animal RNA viral pathogens (Rice, 1996). Virus particles consist of a lipid bilayer envelope with embedded transmembrane glycoproteins surrounding a protein–RNA nucleocapsid. Genome RNAs are single-stranded, of positive polarity, and function as the sole mRNA species for translation of a single long open reading frame (ORF). Mature viral proteins are produced by co- and posttranslational processing of the resulting polyprotein by the action of cellular and viral proteases. Structural proteins destined for incorporation into virus particles are encoded in the N-terminal portion of the polyprotein with the nonstructural proteins which form components of the viral RNA replicase being encoded in the remainder. RNA replication occurs via synthesis of a full-length negative-strand intermediate and is asymmetic, favoring synthesis of positive-strand RNAs.

Besides these common features, the three currently recognized genera of the *Flaviviridae* exhibit distinct differences in transmission, host range, and pathogenesis. Members of the classical flavivirus genus, such as yellow fever virus and dengue virus, are typically transmitted to vertebrate hosts via arthropod vectors and cause acute self-limiting disease (Monath & Heinz, 1996). The pestiviruses, such as bovine viral diarrhea virus (BVDV) and classical swine fever virus (CSFV), cause economically important livestock disease and are spread by direct contact or the fecal-oral route (Thiel et al., 1996). The most recently characterized member of this family is the common and exclusively human pathogen, hepatitis C virus (HCV). HCV, the sole member of the hepacivirus genus, is transmitted by contaminated blood or blood products and is the most common agent of non-A, non-B hepatitis, affecting more that 1% of the population worldwide (Houghton, 1996). Unlike flavivirus and pestivirus infections, which are usually eliminated by host immune response, chronic HCV infections are common and can cause mild to severe liver disease including cancer.

Reprint requests to: Charles M. Rice, Department of Molecular Microbiology, Washington University School of Medicine, Campus Box 8230, 660 South Euclid Avenue, St. Louis, Missouri, 63110-1093, USA; e-mail: rice@borcim.wustl.edu.

[1]The contributions of these authors are considered equal.

[2]Present address: Institute for Molecular Virology, University of Wisconsin, Madison, Wisconsin 53706, USA.

Despite the importance of this virus family, little is known about the details of how RNA replication occurs. For all three genera, full-length functional cDNA clones have been constructed and RNAs transcribed from these cDNA templates are infectious (Ruggli & Rice, 1998). For flaviviruses and pestiviruses, mutagenesis of these clones and efficient RNA transfection of permissive cell cultures provides a means of probing the role of *cis* RNA elements and viral proteins in replicase assembly and function. Such analyses are not yet possible for HCV since this virus is unable to replicate efficiently in cell culture.

Like many other RNA viruses (Huang, 1997), the 5′ and 3′ terminal sequences of the *Flaviviridae* are thought to contain conserved *cis*-elements important for translation, RNA replication, and packaging (Bukh et al., 1992; Deng & Brock, 1993; Cahour et al., 1995; Kolykhalov et al., 1996; Men et al., 1996; Tanaka et al., 1996; Mandl et al., 1998). The 5′ nontranslated region (NTR) functions initially at the level of translation. Similar to most cellular mRNAs, flavivirus genome RNAs are translated in a cap-dependent manner. These RNAs contain a 5′ cap structure that is presumably added by virus-encoded RNA triphosphatases, guanylyl-, and methyltransferases (Rice, 1996). In contrast, the pestiviruses and HCV use a distinct translational strategy more similar to picornaviruses. These RNAs appear to be uncapped and contain long 5′ NTRs with *cis* RNA elements that function as internal ribosome entry sites (IRES) for translation initation at the polyprotein AUG (Lemon & Honda, 1997). Despite containing only short stretches of high sequence identity, the 5′ NTRs of HCV and BVDV have similar structural and functional organization (Wang & Siddiqui, 1995; Lemon & Honda, 1997). The IRES within each NTR is located at the 3′ end of the NTR at a position proximal to the AUG initiation codon of the ORF. Although the 5′ terminal sequence of each of these viruses is apparently not required for IRES function (Rijnbrand et al., 1995; Honda et al., 1996b; Rijnbrand et al., 1997), these sequences are highly conserved among different strains of HCV (Bukh et al., 1992) or BVDV (Deng & Brock, 1993) suggesting other roles in viral replication. Besides their importance in translation initiation, sequences in the 5′ NTR may be required for regulating translation versus initation of negative-strand RNA synthesis. This could occur by direct interaction of 5′ and 3′ RNA elements or indirectly, via RNA-protein interactions. Sequences in the 5′ NTR may also modulate packaging versus translation. Finally, sequences complementary to the 5′ NTR, located at the 3′ end of negative-strand RNA, are likely to function in the initiation of positive-strand RNA synthesis.

In this report, we have used a functional clone of BVDV (Mendez et al., 1998) to construct and characterize a series of 5′ NTR chimeras with sequences derived from HCV and the picornavirus, encephalomyocarditis virus (EMCV). Our results help to define the requirements of a functional BVDV 5′ NTR and provide replication-competent BVDV–HCV chimeras dependent on a functional HCV IRES.

RESULTS

Features of the BVDV, HCV, and EMCV 5′ NTRs important for chimera design

Schematic representations of the proposed secondary structures of the 5′ NTRs of HCV, BVDV, and EMCV are shown, and the location of each IRES is indicated in Figure 1. EMCV is a member of the cardiovirus genus within the family *Picornaviridae*. While not a member of the *Flaviviridae*, EMCV is similar to HCV and BVDV in that it is a positive-strand RNA virus shown to contain an IRES within its 5′ NTR (Jang et al., 1988). Based on their proposed secondary structures, the HCV IRES and the BVDV IRES have been classified as type 3 IRESs, while the EMCV IRES is classified as a type 2 IRES (Lemon & Honda, 1997). However, these three IRESs as well as IRESs from other members of the *Flaviviridae* and the *Picornaviridae* have been proposed to contain a common structural core (Le et al., 1996).

The model for the secondary structure of the 341-nt HCV 5′ NTR has been refined by enzymatic and chemical analysis of synthetic transcripts (Brown et al., 1992; Wang et al., 1994; Honda et al., 1996a; Lima et al., 1997). This element contains four discreet hairpins (referred to here as H1, H2, H3 and H4) and a pseudoknot at the base of hairpin H3 (Wang et al., 1995). The secondary structure of the 385-nt BVDV 5′ NTR has not been as extensively studied, but is proposed to be similar to that of HCV (Brown et al., 1992) with four discrete hairpins (referred to here as B1′, B1, B2, and B3) and a pseudoknot at the base of B3 (Rijnbrand et al., 1997). The secondary structure of the longer (>700 nt) EMCV 5′ NTR consists of a series of hairpins A–M (Duke et al., 1992; Hoffman & Palmenberg, 1996). Recently, a revised model of the EMCV 5′ NTR suggests moderately different secondary structures for the C and G subregions, and significantly different secondary structures for the I–M subregion (Palmenberg & Sgro, 1997).

For HCV, H1 is nonessential for IRES function (Reynolds et al., 1995; Rijnbrand et al., 1995; Honda et al., 1996b; Reynolds et al., 1996; Kamoshita et al., 1997) and its deletion has actually increased translation efficiency in some analyses (Rijnbrand et al., 1995; Honda et al., 1996b). Most studies have found that hairpin H2 and H3 and the pseudoknot are essential for IRES function (Wang et al., 1993; Rijnbrand et al., 1995; Honda et al., 1996b). However, two studies indicate that H2 may not be essential (Tsukiyama-Kohara et al., 1992; Urabe et al., 1997). The 3′ boundary of the HCV

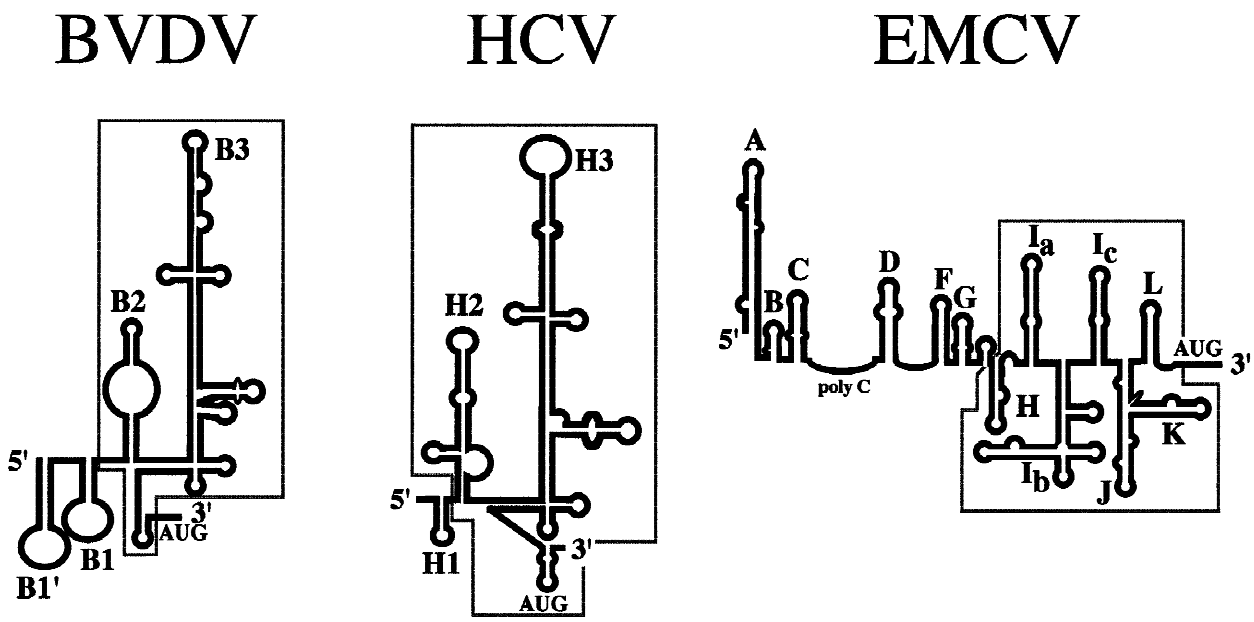

FIGURE 1. Schematic representation of the 5′ NTRs of BVDV, HCV, and EMCV. The position of the start codons of the ORF are indicated, and the canonical IRES elements are boxed.

IRES is more controversial. The IRES clearly extends to the AUG initiation codon. However, some studies indicate that sequences affecting the efficiency of translation initiation extend into the ORF (Reynolds et al., 1995; Honda et al., 1996a; Honda et al., 1996b; Lu & Wimmer, 1996). By analogy to the HCV IRES and the related pestivirus CSFV IRES, the BVDV IRES probably requires hairpins B2 and B3 and the pseudoknot for function, with B1′ and B1 probably not required for IRES activity (Poole et al., 1995; Rijnbrand et al., 1997). For EMCV, hairpins H–L have been shown to be required for IRES function in mono- or dicistronic constructs (Jang & Wimmer, 1990; Duke et al., 1992). The remaining portion of the EMCV 5′ NTR is thought to be required for RNA replication or unknown steps in viral replication that are important for pathogenesis (Duke et al., 1990; Martin & Palmenberg, 1996).

Replacement of the BVDV 5′ NTR with the HCV 5′ NTR results in a large decrease in specific infectivity

Since the BVDV 5′ NTR and the HCV 5′ NTR are proposed to have similar RNA secondary structure and functional organization, we tested whether the BVDV 5′ NTR could be replaced by the HCV 5′ NTR. p5′HCV has an exact replacement of the BVDV 5′ NTR with that of HCV (Fig. 2A), while the coding sequence and 3′ NTR of p5′HCV are identical to pBVDV. Positioning of the HCV 5′ NTR in such a manner was necessary since translation initiation from the HCV IRES begins at or near the AUG start codon (Honda et al., 1996a; Reynolds et al., 1995; Reynolds et al., 1996; Rijnbrand et al., 1996). The specific infectivity of 5′HCV RNA synthesized in vitro was compared to that of BVDV RNA by transfection of MDBK (bovine kidney) cells (Fig. 2A). The specific infectivity of BVDV RNA was approximately 4×10^6 plaque forming units (PFU)/μg RNA. In contrast, the specific infectivity of 5′HCV RNA was near the limit of detection (30–50 PFU/μg RNA) and considerable plaque heterogeneity was apparent. These results suggested that the HCV 5′ NTR replacement chimera might be incapable of efficient replication and plaque formation and that the plaque forming virus observed had arisen by secondary mutation(s). Sequence analysis of plaque-purified 5′HCV viruses presented below confirmed that the replicating pool of virus contained such pseudorevertants.

We next analyzed the in vitro translation efficiency of these two RNAs in rabbit reticulocyte extracts to test whether the defect in specific infectivity of 5′HCV RNA could be attributed to lower translation efficiency. Although the specific infectivity of 5′HCV RNA was reduced ~5 logs compared to BVDV RNA, its translation efficiency was only slightly reduced, ~twofold (Fig. 3, lane 1 vs. lane 2). The apparent size of the N-terminal cleavage product, N^{pro}, was identical for both RNAs suggesting that translation initiated with the correct AUG. These data are consistent with the hypothesis that the BVDV 5′ NTR contains signals that are required for a step in replication other than translation which are not present in the 5′HCV chimera.

Given the low specific infectivity of 5′HCV RNA, we next tested the effect of placing the BVDV 5′ NTR sequence upstream of the HCV 5′ NTR, resulting in tandem BVDV and HCV 5′ NTRs (called BVDV+HCV).

This arrangement actually decreased translation efficiency (Fig. 3, lane 14 vs. lane 1) yet restored infectivity (Fig. 2A). The plaques produced by BVDV+HCV were also heterogeneous in size, indicating that this virus was unstable. Upon passage, RT-PCR analysis indicated that pseudorevertants had indeed arisen in which portions of the BVDV and/or HCV 5′ NTRs had been deleted (data not shown). These data show that sequences in the BVDV 5′ NTR required for virus replication can function when placed upstream of a functional HCV IRES driving translation of the BVDV polyprotein.

Hairpins B1′ and B1 in conjunction with the HCV IRES are sufficient for stable and efficient BVDV replication

We next attempted to map the sequences within the BVDV 5′ NTR that restored replication in the context of the HCV 5′ NTR. To do so we used three deletion variants. The deletion BVDV+HCVdelB3 removed a large portion of hairpin B3; the deletion within BVDV+HCVdelB2B3 removed hairpins B2 and B3, and the deletion within BVDV+HCVdelB1B2B3 removed hairpins B1, B2 and B3. The specific infectivities of RNAs from these deletion mutants were near that of BVDV RNA (Fig. 2). Upon passage of these viruses, RT-PCR analyses and sequencing indicated that BVDV+HCVdelB3 and BVDV+HCVdelB2B3 were stably propagated and produced homogeneous plaques slightly smaller than those of wild-type BVDV (data not shown). In contrast, BVDV+HCVdelB1B2B3 produced smaller heterogeneous plaques. Reverse transcription–polymerase chain reaction (RT-PCR) analysis and sequencing indicated that BVDV+HCVdelB1B2B3 underwent a reversion event described in more detail below. The translation efficiencies of these three RNAs (Fig. 3, lanes 9, 10, and 12) were similar to BVDV+HCV RNA (Fig. 3, lane 14), indicating that the deleted portions (hairpins B1, B2, and B3) are not required for translation in the BVDV+HCV chimera. These results show that B1′ and B1 are the minimal elements sufficient for stable replication in conjunction with the HCV 5′ NTR.

Having shown that B1′ and B1 are sufficient for replication in conjunction with the HCV 5′ NTR, we next conducted a deletion analysis to determine the sequences within the HCV 5′ NTR of BVDV+HCVdelB2B3 required for replication. A large portion of H1 was deleted in BVDV+HCVdelB2B3H1, while both H1 and H2 were deleted in BVDV+HCVdelB2B3H1H2. Of these two RNAs, only BVDV+HCVdelB2B3H1 was as infectious as parental BVDV RNA (Fig. 2B). However, the BVDV+HCVdelB2B3H1 virus produced smaller plaques than BVDV+HCVdelB2B3, indicating that hairpin H1 may augment replication of the chimera. In contrast, BVDV+HCVdelB2B3H1H2 RNA was not infectious (Fig. 2B) and was translated poorly (Fig. 3, lane 11). Diminished HCV IRES activity might be due to deletion of hairpin H2 or juxtaposition of BVDV hairpins B1′ and B1 with H3. A third derivative of BVDV+HCVdelB2B3, with a *Sma* I–*Sma* I deletion abrogating HCV IRES function by removing H3, was also not infectious (data not shown). Thus, a 5′ NTR consisting of B1′ and B1 and a functional HCV IRES is sufficient for stable BVDV replication in MDBK cells. Similar results were obtained in BT cells, another BVDV-permissive continuous bovine cell line (data not shown).

Replacement of the BVDV 5′ NTR with the EMCV 5′ NTR

We next attempted to determine whether the BVDV 5′ NTR could be replaced by the 5′ NTR of a more phylogenetically distant virus, EMCV. We created a derivative of BVDV called 5′EMCV (Fig. 4A), that contains an exact replacement of the BVDV 5′ NTR with the EMCV 5′ NTR plus an additional guanosine residue at the 5′ terminus for more efficient transcription initiation by T7 polymerase. The specific infectivity of 5′EMCV RNA was more than three orders of magnitude lower than BVDV RNA, indicating that it was defective for replication, although its specific infectivity was higher than that of 5′HCV RNA (compare Figs. 4A and 2A). Similar to 5′HCV, 5′EMCV produced heterogeneous plaques, and sequence analysis indicated that pseudorevertants had arisen. The lower specific infectivity of 5′EMCV RNA was not likely because of a defect in translation, since the translation efficiency of 5′EMCV RNA was about threefold higher in vitro than that of BVDV RNA (Fig. 3, lane 20 vs. lane 19).

Similar to BVDV+HCV, we tested whether placing the BVDV 5′ NTR at the 5′ end of the 5′EMCV RNA would increase its specific infectivity. BVDV+EMCVdelA (Fig. 4A) contained the entire BVDV 5′ NTR in tandem with the EMCV 5′ NTR lacking a portion of hairpin A. BVDV+EMCVdelA RNA had a specific infectivity near that of BVDV RNA (compare Figs. 4A and 2A) despite having a lower translation efficiency than 5′EMCV (Fig. 3, lane 21 vs. lane 20). Similar to the results with BVDV+HCV, this implicates the added BVDV 5′ NTR sequence for a step in viral replication other than translation. Two derivatives of BVDV+EMCVdelA that contain deletions of portions of the BVDV 5′ NTR but maintain the sequence of B1′ and B1, BVDV+EMCVdelB3A and BVDV+EMCVdelB2B3A (Fig. 4A), also were infectious. These derivatives had translation efficiencies near that of the parental BVDV+EMCVdelA (Fig. 3, compare lanes 15 and 16 with lane 21). This demonstrated that hairpins B1′ and B1 were sufficient for replication in conjunction with a large portion of the EMCV 5′ NTR. Derivatives of BVDV+EMCVdelB3A

A

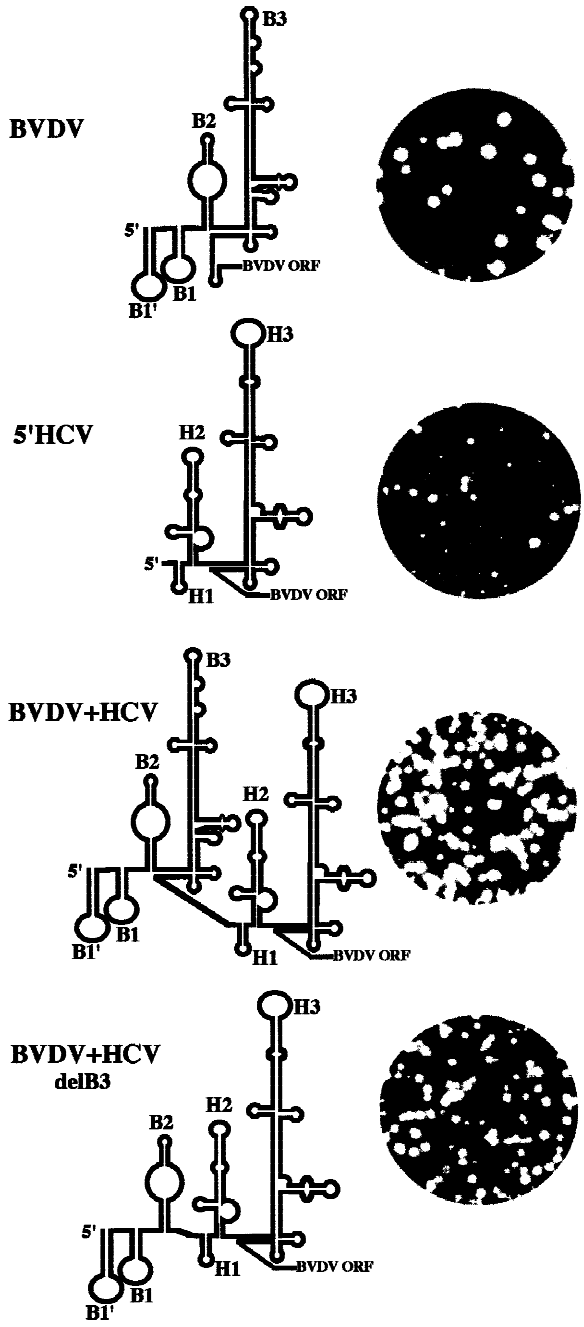

	Translation efficiency (% of BVDV)	Infectivity (PFU/μg of RNA)	Virus titer (PFU/ml) 24h	Virus titer (PFU/ml) 48h	Pseudorevertants
BVDV	100	4×10^6	1×10^8	8×10^7	No
5'HCV	50	30-50	<50	4×10^5 (72 h)	Yes
BVDV+HCV	25	5×10^6	1×10^8	1×10^8	Yes
BVDV+HCV delB3	16	4×10^6	7×10^7	1×10^8	N.D.

FIGURE 2. Schematic representation of BVDV and HCV chimeras, plaque phenotypes, reticulocyte translation efficiencies relative to parental BVDV, specific infectivities in MDBK cells, titers at 24 and 48 h post-transfection (or 72 h, as indicated), and an indication of whether pseudorevertants arose. **A**: BVDV, 5′HCV, BVDV+HCV, and BVDV+HCVdelB3. **B**: BVDV+HCVdelB2B3, BVDV+HCVdelB1B2B3, BVDV+HCVdelB2B3H1, and BVDV+HCVdelB2B3H1H2. N.D.: not determined. (*Figure continues on facing page.*)

or BVDV+EMCVdelB2B3A that contain further deletions of EMCV (BVDV+EMCVdelB3ABC and BVDV+EMCVdelB2B3ABC in particular) were translated efficiently (Fig. 3, lanes 17 and 18) and were infectious (Fig. 4B). This indicates that the chimeras did not require putative EMCV RNA replication signals (Martin & Palmenberg, 1996). However, derivatives with deletions extending into the canonical EMCV IRES were not infectious. For example, BVDV+EMCVdelB3A-H and BVDV+EMCVdelB2B3A-H, in which a portion of hairpin H is deleted, were not infectious (Fig. 4B) and were inefficiently translated in vitro (Fig. 3, lanes 22

B

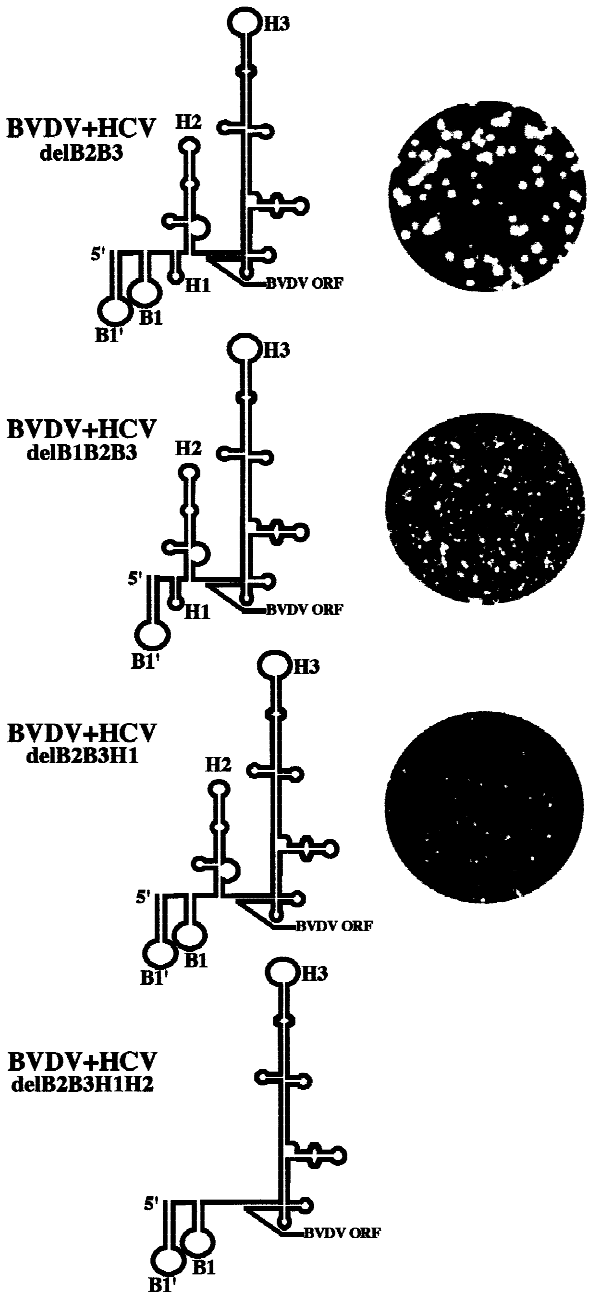

Translation efficiency (% of BVDV)	Infectivity (PFU/μg of RNA)	Virus titer (PFU/ml) 24h	Virus titer (PFU/ml) 48h	Pseudorevertants
24	3×10^6	7×10^7	1×10^8	N.D.
29	3×10^6	1×10^7	8×10^7	Yes
24	2×10^6	2×10^7	1×10^8	N.D.
3	0	<50	<50	N.D.

FIGURE 2. (*Continued.*)

and 23). It should be noted that all of the BVDV+EMCV chimeras produced plaques of heterogeneous size, indicating some instability.

Relatively simple 5′ NTR mutations are observed in adapted pseudorevertants

As mentioned previously, BVDV+HCVdelB1B2B3 did not replicate stably as indicated by the heterogeneity in the size of plaques produced by this virus. Upon passage and selection of medium plaque-producing variants, 5′ RACE analysis and sequencing indicated that nt 1–26 had been deleted in the pseudorevertants, removing a large portion of B1′ which was apparently deleterious in the absence of B1. This deletion results in the 5′ terminal sequence 5′-GUAUCG which is identical to the first six bases of BVDV genome RNA (Fig. 5) and is repeated at positions 27–32.

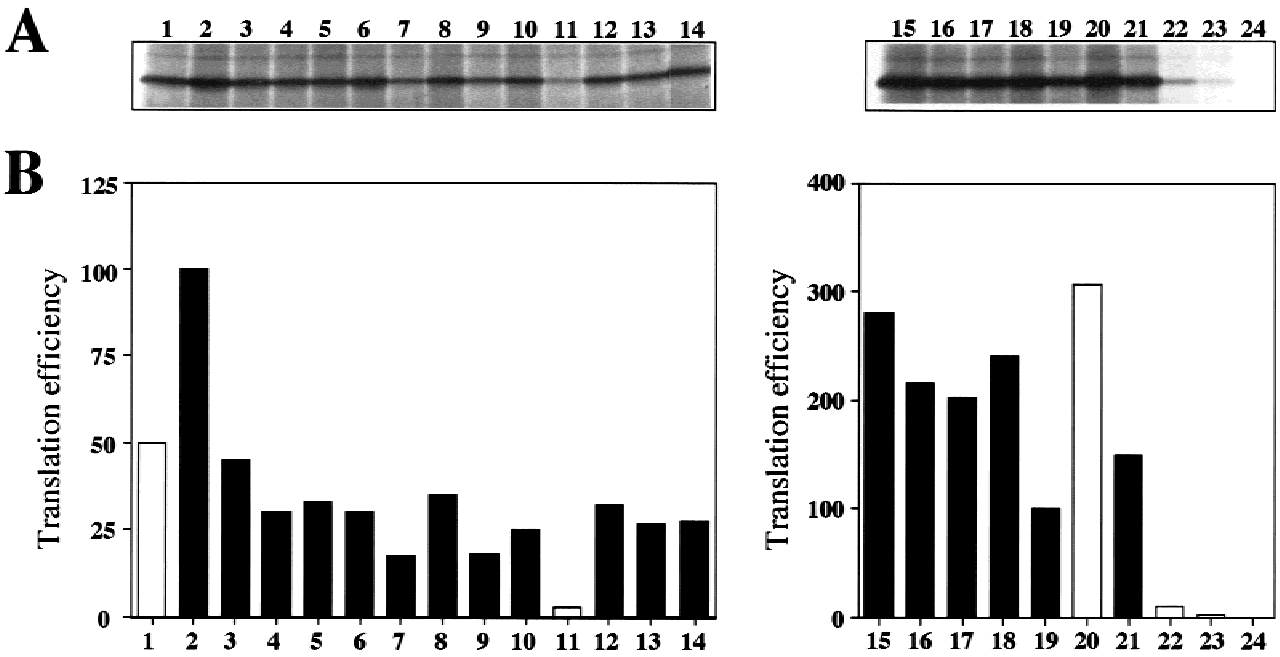

FIGURE 3. In vitro translation efficiency of BVDV RNA or chimeras. Translations were performed at 30 °C for 45 min in 25-μl reaction mixtures using subsaturating amounts (0.4 μg) of in vitro synthesized RNAs. Two μl of the reactions were diluted in 10 μl of sample buffer and loaded on 10% sodium dodecyl sulfate-polyacrylamide gels. Labeled proteins were visualized by autoradiography of the dried gel. Only the portions of the gels containing N^{pro}, the N-terminal protein in the BVDV ORF, are shown in (**A**). **B**: The efficiency of translation was measured by phosphorimager analysis (Molecular Dynamics) by comparing the radioactivity in the band corresponding to N^{pro}. The background was measured separately for each lane and subtracted, and the translation efficiency normalized with respect to BVDV RNA is indicated. Filled bars are used to indicate RNAs that were clearly infectious (specific infectivities $> 4 \times 10^5$ PFU/μg RNA). Open bars indicate noninfectious RNAs. 5′HCV, lane 1; BVDV, lane 2 and 19; 5′HCV.R1orig, lane 3; 5′HCV.R1cons, lane 4; 5′HCV.R3orig, lane 5; 5′HCV.R3cons, lane 6; 5′HCV.R2orig, lane 7; 5′HCV.R2cons, lane 8; BVDV+HCVdelB3, lane 9; BVDV+HCVdelB2B3, lane 10; BVDV+HCVdelB2B3H1H2, lane 11; BVDV+HCVdelB1B2B3, lane 12; BVDV+HCVdelB2B3H1, lane 13; BVDV+HCV, lane 14; BVDV+EMCVdelB3A, lane 15; BVDV+EMCVdelB2B3A, lane 16; BVDV+EMCVdelB3ABC, lane 17; BVDV+EMCVdelB2B3ABC, lane 18; 5′EMCV, lane 20; BVDV+EMCVdelA, lane 21; BVDV+EMCVdelB3A-H, lane 22; BVDV+EMCVdelB2B3A-H, lane 23; no RNA, lane 24.

Analysis of the passaged 5′EMCV virus indicated that the replicating progeny had also undergone a simple deletion of sequence at the 5′ end to generate more efficiently replicating variants (Fig. 5). After electroporation, the 5′EMCV virus pool was passaged 5 times at a multiplicity of infection of 0.1–1 PFU/cell on MDBK or BT cells, and the 5′ termini of three randomly picked plaques were sequenced. For all three plaques selected, nt 2–209 had been deleted, again creating a genome RNA with the 5′ terminal tetranucleotide sequence 5′-GUAU.

Analysis of the 5′HCV progeny indicated that more complicated variants had arisen. Most small plaque-producing variants were unstable and quickly reverted to medium plaque-producing variants. However, we were able to isolate one small plaque-producing variant, and in addition, we isolated two stable medium plaque-producing variants. 5′ terminal sequences of the variants were amplified by rapid amplification of cDNA ends (RACE) and cloned into a plasmid vector, and sequences for several independent colonies were determined. The sequence of three clones of the small plaque-producing virus (5′HCV.R1) contained a deletion of HCV sequence from nt 1–34 and an addition of the dinucleotides 5′-AU in two clones and 5′-GU in the third clone. This creates a 5′ terminus of 5′-(G/A)UAA (Fig. 5B), reminiscent of the first three bases of the BVDV genome RNA (5′-GUA). Both medium plaque variants appeared to have arisen by RNA recombination with non-viral sequences (Fig. 5). One medium plaque variant (5′HCV.R2) had deleted the first 21 bases of the HCV sequence and contained instead a heterologous sequence of 22 bases. BLAST searches revealed a perfect match between this sequence and a sequence in a human retina cDNA of unknown function (Tsp509I). The second medium plaque variant (5′HCV.R3) had also undergone a possible recombination event leading to the addition of 12 nt to the 5′ end of the HCV sequence. Given its short length, multiple matches were found in the database with this sequence. As for the small plaque variant, sequencing of multiple clones revealed heterogeneity at the extreme 5′ end, with either G or A identified as the 5′ base. Remarkably, for both medium plaque variants, the fused heterologous sequence began with the tetranucelotide sequence 5′-(G/A)UAU (Fig. 5B). For all three variants, sequenc-

ing of the entire 5′ NTR and a portion of the N^{pro} coding region revealed only these changes at the 5′ termini.

5′ NTR sequence changes are sufficient for the pseudorevertant phenotypes

To assess the importance of these alterations at the 5′ terminus of the 5′HCV pseudorevertants, we created derivatives of 5′HCV with the changes determined by 5′ RACE (Fig. 6A) and analyzed the specific infectivities of these RNAs (Fig. 6B). Corresponding to the small plaque variant, we engineered a derivative called 5′HCV.R1orig with a 5′ NTR consisting of the dinucleotide 5′-GU at the 5′ terminus of HCV nt 35–341. This results in a 5′ terminus consisting of 5′-GUAA. 5′HCV.R1orig RNA had a specific infectivity at least four orders of magnitude higher than 5′HCV RNA (Figs. 6B and 2A). This demonstrates that this 5′ NTR structure is sufficient for phenotypic reversion to high specific infectivity. However, small plaques and considerable heterogeneity were observed for 5′HCV.R1orig suggesting that additional mutations may be present in the original small plaque variant.

The engineered derivative 5′HCV.R2orig had a 5′ NTR consisting of 22 nt of Tsp509I-homologous sequence followed by HCV nt 22–341. We also constructed 5′HCV.R3orig with the 12 nt of the other heterologous sequence fused to the intact HCV 5′ NTR. Specific infectivities for both these derivatives were essentially the same as observed for wild type BVDV RNA ($2–4 \times 10^6$ PFU/μg; Fig. 6B). Transfection with these transcripts produced medium plaques, as observed for the original variants, and this phenotype was stable upon passaging. These results show that the altered 5′NTR sequences were responsible for the pseudorevertant phenotypes rather than changes elsewhere in their genomes.

Addition of the tetranucleotide sequence 5′-GUAU to the HCV 5′ NTR allows efficient BVDV replication

For all three 5′HCV variants studied, as well as the BVDV+HCVdelB1B2B3 and 5′EMCV pseudorevertants, 5′ NTR alterations seemed to involve creation of a three- or four-base "consensus" sequence identical to the 5′ terminus of BVDV genome RNA. To test the importance of this sequence, as opposed to fused heterologous sequences, we created a set of variants with the BVDV 5′ tetranucleotide sequence linked to the HCV 5′ NTR or the deletion/recombinant break points identified during sequence analysis of the 5′HCV pseudorevertants (Fig. 6A). 5′HCV.R1cons had the tetranucleotide sequence 5′-GUAU fused to HCV nt 35–341. 5′HCV.R2cons had the 5′-GUAU tetranucleotide sequence fused to HCV nt 22–341. 5′HCV.R3cons contained the tetranucleotide sequence 5′-GUAU fused to the intact 5′ terminus of the HCV NTR. RNAs from all three of these derivatives had specific infectivities more than five orders of magnitude higher than 5′HCV and comparable to parental BVDV (Fig. 6B).

There were, however, significant differences between the phenotypes of some of these derivatives versus the reconstructed pseudorevertants. As mentioned above, 5′HCV.R1orig yielded tiny and small plaques and produced low virus yields even after 48 h. In contrast, the addition of four bases rather than two bases (5′-GUAU vs. 5′-GU) yielded virus with near wild-type plaque morphology (Fig. 6B) and growth rates (Fig. 7). In the case of the smaller deletion, 5′HCV.R2orig and 5′HCV.R2cons were indistinguishable, suggesting that, other than the 5′ four bases, the fused heterologous sequences were dispensable. This was not the case, however, for the chimera containing the 5′-GUAU tetranucleotide sequence fused to the intact HCV 5′ NTR. 5′HCV.R3cons produced small plaques (Fig. 6B) and grew more slowly than 5′HCV.R3orig (Fig. 7) suggesting that the sequence/structure of the sequences downstream of the 5′ four bases can affect replication efficiency.

The tetranucleotide sequence 5′-GUAU is important for efficient BVDV RNA accumulation

We next analyzed the effects of the different 5′ termini on virus-specific RNA accumulation directly after transfection. This allowed a direct comparison between 5′HCV and the reconstructed pseudorevertants as well as selected BVDV+HCV deletion constructs. MDBK cells were transfected with in vitro synthesized RNAs and labeled for 10 h beginning at 6 h post-transfection with ^{3}H-UTP in the presence of actinomycin D (Fig. 8). RNA replication of the 5′HCV chimera was severely impaired to a level below detection (Fig. 8, lane 2). In contrast, every 5′ NTR alteration of 5′HCV that increased RNA specific infectivity and allowed efficient virus growth led to readily detectable viral RNA accumulation. Addition of B1′ and B1 to the 5′ terminus of the HCV 5′ NTR restored RNA replication to a level ~50% of that observed for BVDV (BVDV+HCVdelB2B3; Fig. 8, lane 3 vs. lane 1). BVDV+HCVdelB2B3H1 displayed reduced RNA synthesis compared to BVDV+HCVdelB2B3 (Fig. 8, lane 4 vs. lane 3) perhaps explaining its small plaque phenotype and suggesting a possible positive role for H1 in replication of this chimera. 5′HCV.R1orig, which had exhibited plaque heterogeneity and slow growth, accumulated less RNA when compared to 5′HCV.R1cons (Fig. 8, lane 5 vs. lane 6). 5′HCV.R2orig and 5′HCV.R2cons showed similar RNA accumulation (Fig. 8, lane 9 vs. lane 10) consistent with their medium plaque phenotypes; and 5′HCV.R3cons exhibited re-

A

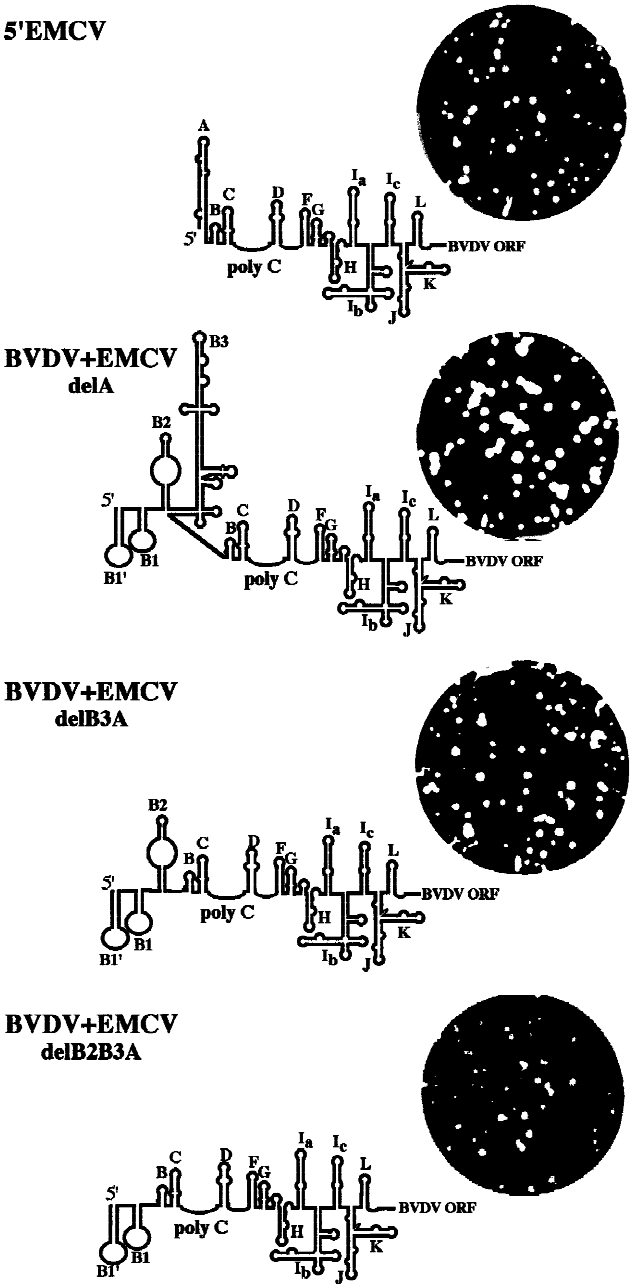

Translation efficiency (% of BVDV)	Infectivity (PFU/μg of RNA)	Virus titer (PFU/ml) 24h	Virus titer (PFU/ml) 48h	Pseudorevertants
307	$2x10^3$	$5x10^2$	$3x10^6$ (72h)	Yes
153	$3x10^6$	$6x10^6$	$6x10^7$	Yes
280	$2x10^6$	$5x10^5$	$7x10^7$	Yes
216	$4x10^6$	$6x10^5$	$5x10^7$	Yes

FIGURE 4. Schematic representation of EMCV chimeras, plaque phenotypes, reticulocyte translation efficiencies relative to parental BVDV, specific infectivities in MDBK cells, titers at 24 and 48 h post-transfection (or 72 h, as indicated), and an indication of whether pseudorevertants arose. **A**: 5′EMCV, BVDV+EMCVdelA, BVDV+EMCVdelB3A, and BVDV+EMCVdelB2B3A. **B**: BVDV+EMCVdelB3ABC, BVDV+EMCVdelB2B3ABC, BVDV+EMCVdelB3A-H, and BVDV+EMCVdelB2B3A-H. (*Figure continues on facing page.*)

duced RNA synthesis compared to 5′HCV.R3orig (Fig. 8, lane 8 vs. lane 7), consistent with their small- versus medium-plaque phenotypes.

Although these RNA phenotypes are complex, the most striking result is that addition of the B1′ B1 hairpins, addition of heterologous 5′ sequences terminating with 5′-GUAU or simply fusion of this tetranucleotide sequence with the HCV 5′ NTR or short 5′ truncations of the HCV 5′ NTR all dramatically upregulated RNA accumulation. This occurred without increasing trans-

B

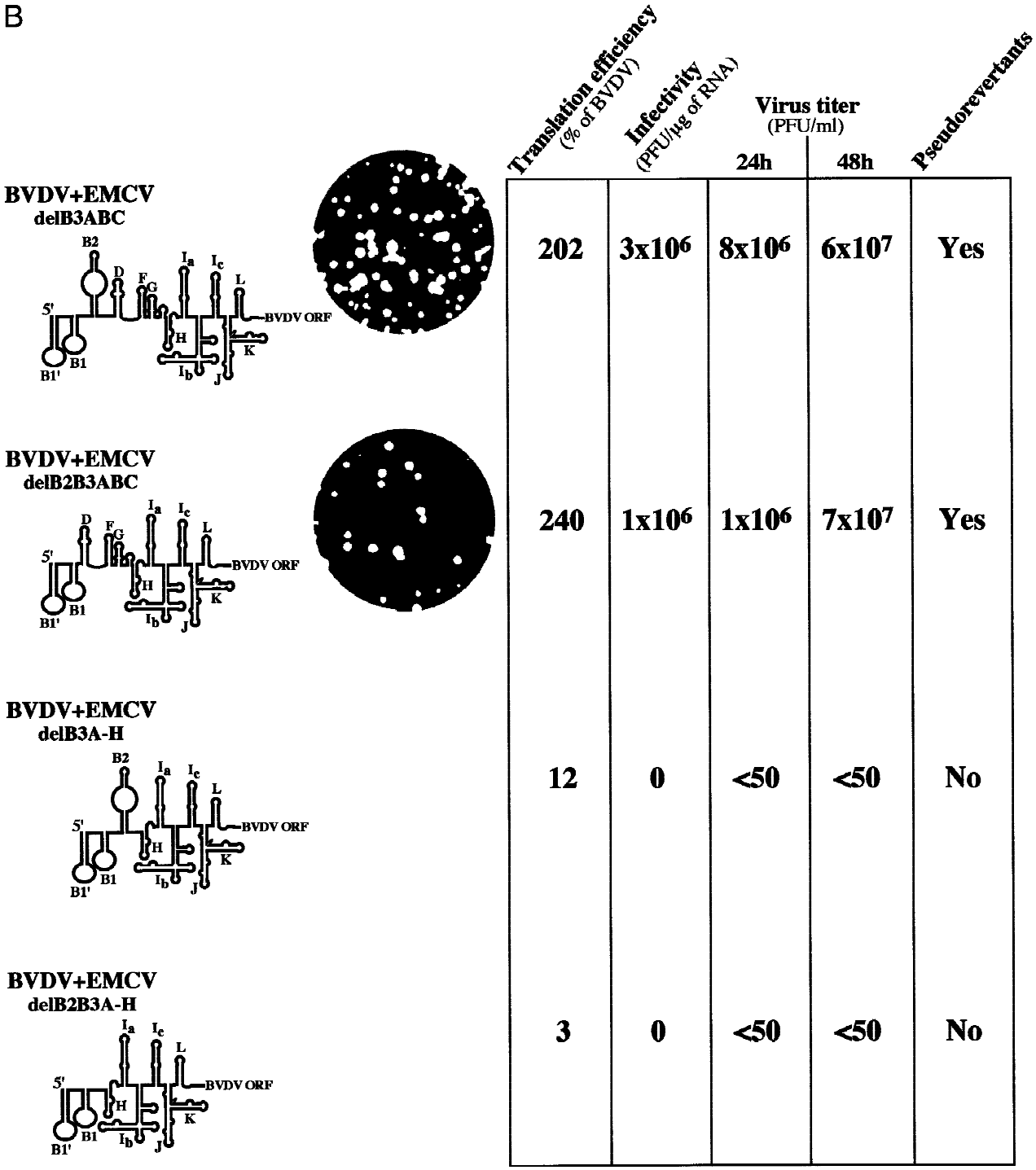

FIGURE 4. (*Continued.*)

lation efficiency, at least as measured in a cell-free assay (Fig. 3, compare lanes 3–8 to lane 1), suggesting that these sequences function at the level of RNA replication or stability.

DISCUSSION

The work presented here helps to define the requirements for a functional BVDV 5′ NTR. The BVDV-specific 5′ NTR sequences required for efficient replication in cell culture are minimal and consist of the 5′ terminal sequence, 5′-GUAU. The sequence 5′-AUAU, detected for some pseudorevertants, may also be functional but this was not tested for technical reasons. This simple 5′-terminal tetranucleotide sequence, which is conserved among pestivirses (Ruggli et al., 1996; Becher et al., 1998), was shown to function in the context of functional IRES elements derived from the hepacivirus

A

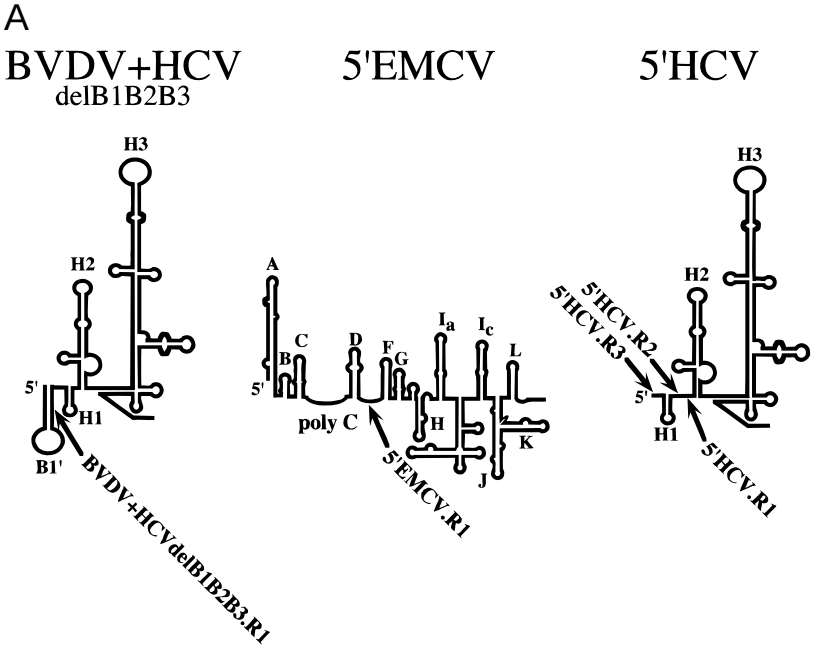

B

BVDV+HCVdelB1B2B3

```
                                <              B1'             >                <      H1      >
BVDV+HCVdelB1B2B3    guauacgagaauuagaaaaggcacucguauacguaCAUGGCACGUgccagccccccugaugggggc
BVDV+HCVdelB1B2B3.R1                                guauacguaCAUGGCACGUgccagccccccugaugggggc
```

5'HCV

```
                                          <      H1      >                        <      H2
5'HCV                                gccagccccccugaugggggcgacacuccaccaugaaucacuccccugugaggaac
5'HCV.R1                                                          (G/A)Uaaucacuccccugugaggaac
5'HCV.R2                       (G/A)UAUCAGAAGUGCGAAUGCUGAacacuccaccaugaaucacuccccugugaggaac
5'HCV.R3          (G/A)UAUUGCAGUUUgccagccccccugaugggggcgacacuccaccaugaaucacuccccugugaggaac
```

5'EMCV

```
                  1                                                  201
5'EMCV       guugaaagccggggguggg·····················  ··guuugucuauauguuauuuuccaccauauug
5'EMCV.R1                                                          Guauguuauuuuccaccauauug
```

FIGURE 5. Pseudorevertant analyses. **A**: Relative positions of mutations detected within the plaque-purified variants of passaged BVDV+HCVdelB1B2B3, 5′EMCV, and 5′HCV. **B**: 5′ terminal sequences of pseudorevertants of BVDV+HCVdelB1B2B3, 5′EMCV, and 5′HCV. Novel nucleotides or sequences are shown in bold upper case type. Pseudorevertants are numbered and designated by the suffix ".R". The upper case sequence in BVDV+HCVdelB1B2B3 and BVDV+HCVdelB1B2B3.R1 is a remnant of downstream BVDV 5′ NTR sequences and was created during the cloning procedures.

HCV or the picornavirus EMCV. As discussed below, this may indicate that the 5′ signals required for BVDV RNA replication are rather simple or that elements in these heterologous IRESs can functionally replace deleted BVDV sequences.

Sequences at the extreme 5′ end of BVDV genome RNA could modulate the efficiency of RNA accumulation by affecting RNA stability, translation, promoter efficiency, or some combination of these processes. At this time, we can not distinguish among these possibilities but favor an effect on RNA replication. The complement of the BVDV 5′ sequence at the 3′ end of negative-strand RNA presumably functions in the initiation of positive-strand RNA synthesis. Thus, AUAC-3′ at the 3-terminus of minus-strand RNA may be important for positive-strand RNA synthesis. Interestingly, for

some positive-strand RNA viruses such as rubella virus (Pugachev & Frey, 1998), flock house virus (Ball, 1994) and turnip crinkle virus (Guan et al., 1997), only minimal *cis*-acting sequences at the 3′ termini of negative-strand RNAs are required positive-strand RNA synthesis. In contrast to the 5′ NTR replacements, we were unable to generate replication-competent BVDV–HCV chimeras (or pseudorevertants) with the 3′ NTR of HCV replacing that of BVDV (data not shown). This may indicate that the signals within the pestivirus 3′ NTR required for initiation of negative-strand RNA synthesis are more complex and virus specific. Once the replication complex has assembled at the 3′ NTR and transversed the RNA during negative-strand synthesis, the requirements at the 5′ NTR for initiation of positive-strand synthesis may be minimal.

Although the RNA replication signals within the 5′ NTR appear to be rather simple, we cannot exclude the possibility that the signals important for RNA replication actually extend into the IRES and are more complicated. For instance, our 5′HCV pseudorevertants were more stable and grew to higher titers than the 5′EMCV counterparts, despite the fact that the 5′EMCV RNAs were translated more efficiently in vitro. This may indicate that the BVDV and HCV IRESs contain signals important for RNA synthesis that are absent in the EMCV IRES. Unfortunately, due to technical difficulties we were unable to measure the translation efficiency of the chimeric RNAs directly in MDBK cells capable of supporting BVDV replication using transient expression assays. Thus we cannot exclude the possibility that the translation efficiencies that we observe in vitro do not correlate with the translation efficiencies in infected cells. We have not yet measured the RNA synthesis levels of any of our 5′EMCV pseudorevertants directly, so it may be that they are actually impaired at some other step in viral replication.

It is perhaps not surprising that 5′HCV appeared to recombine with cellular mRNAs to acquire a 5′ terminus with the 5′-(G/A)UAU consensus, given that noncytopathic strains of BVDV can recombine with BVDV RNA or cellular mRNAs to generate cytopathic strains of BVDV (Meyers & Thiel, 1996). Presumably, this recombination event involves template switching during negative-strand RNA synthesis, as observed for poliovirus (Kirkegaard & Baltimore, 1986). In contrast to 5′HCV, simple deletions of 5′ terminal viral sequences could account for the BVDV+HCVdelB1B2B3 and 5′EMCV pseudorevertants since the tetranucleotide sequence is present in these 5′ NTRs upstream of functional IRES elements. Such deletions could occur by partial degradation of positive-strand template prior to negative-strand synthesis, by premature termination during negative-strand RNA synthesis, or by degradation of 3′ terminal negative-strand sequence after synthesis. We hypothesize that 5′HCV was forced to recombine with cellular sequences because HCV does not have an 5′-(G/A)UAU sequence upstream of its IRES. The first occurrence of an (G/A)UAU tetranucleotide sequence is at nt 94–97 within hairpin H2, and a 5′ deletion extending into this sequence would presumably inactivate or severely impair HCV IRES activity. It is interesting that BVDV+HCVdelB1B2B3 and 5′EMCV pseudorevertants were generated at much higher frequency than 5′HCV pseudorevertants. This may indicate that recombination between BVDV and cellular RNAs is a rare event compared to the processes which lead to deletion of terminal viral sequences.

Poliovirus chimeras dependent upon a functional HCV IRES have been reported (Lu & Wimmer, 1996). Interestingly, viable poliovirus chimeras were produced only when HCV sequences included both the IRES and the N-terminal portion of the HCV ORF. Nucleotide sequences or structures in the downstream ORF can modulate HCV IRES translational efficiency (see Reynolds et al., 1995; Honda et al., 1996a) but it was also suggested that the N-terminal portion of the HCV core polypeptide might be involved. In the case of our 5′HCV pseudorevertants, there is no requirement for HCV C protein sequences. Although we have not directly assessed the translation efficiency of the HCV IRES in the presence of additional HCV sequences 3′ to the AUG start, the HCV chimeras and pseudorevertants were translationally active and infectious in the absence of any portion of the HCV ORF. This indicates that either the HCV IRES does not extend into the HCV ORF or that the BVDV ORF contains analogous sequence which functions in our 5′HCV chimeras. There is some limited identity between HCV and BVDV within this region. For example, HCV nt 359–394 and BVDV nt 405–440 are identical at 21 of 36 positions, although identity within this sequence may be attributed to a high adenosine content. It is interesting to note that the luciferase (LUC) and chloramphenicol acetyl transferase (CAT) reporter genes previously used to detect HCV IRES activity (Tsukiyama-Kohara et al., 1992; Wang et al., 1993) also have adenosine- or purine-rich regions in relatively the same position as the HCV ORF and BVDV ORF. If this region is indeed important for IRES activity, this may explain why some have observed that the HCV IRES does not require a portion of the HCV ORF for translation of CAT or LUC (Tsukiyama-Kohara et al., 1992; Wang et al., 1993). Point mutations and insertions within this region of HCV have been shown to reduce HCV IRES activity in vitro (Honda et al., 1996a,b).

Despite the fact that B1′ and B1 are conserved among different strains of BVDV and similar hairpins are present in border disease virus and CSFV (Deng & Brock, 1993; Becher et al., 1998), B1′ and B1 were dispensable for BVDV replication, provided that the 5′ tetranucleotide sequence 5′-(G/A)UAU remained. This may indicate a role for B1′ and B1 in viral replication in vivo that we do not observe in cell culture. It will be interesting to test

A

```
5'HCV                gccagccccugaugggggcgacacuccaccaugaaucacuccccugugaggaacu
5'HCV.R1orig                                GUaaucacuccccugugaggaacu
5'HCV.R1cons                                GUAUaaucacuccccugugaggaacu
5'HCV.R2orig         GUAUCAGAAGUGCGAAUGCUGAacacuccaccaugaaucacuccccugugaggaacu
5'HCV.R2cons                                GUAUacacuccaccaugaaucacuccccugugaggaacu
5'HCV.R3orig     GUAUUGCAGUUUgccagccccugaugggggcgacacuccaccaugaaucacuccccugugaggaacu
5'HCV.R3cons                GUAUgccagccccugaugggggcgacacuccaccaugaaucacuccccugugaggaacu
```

B

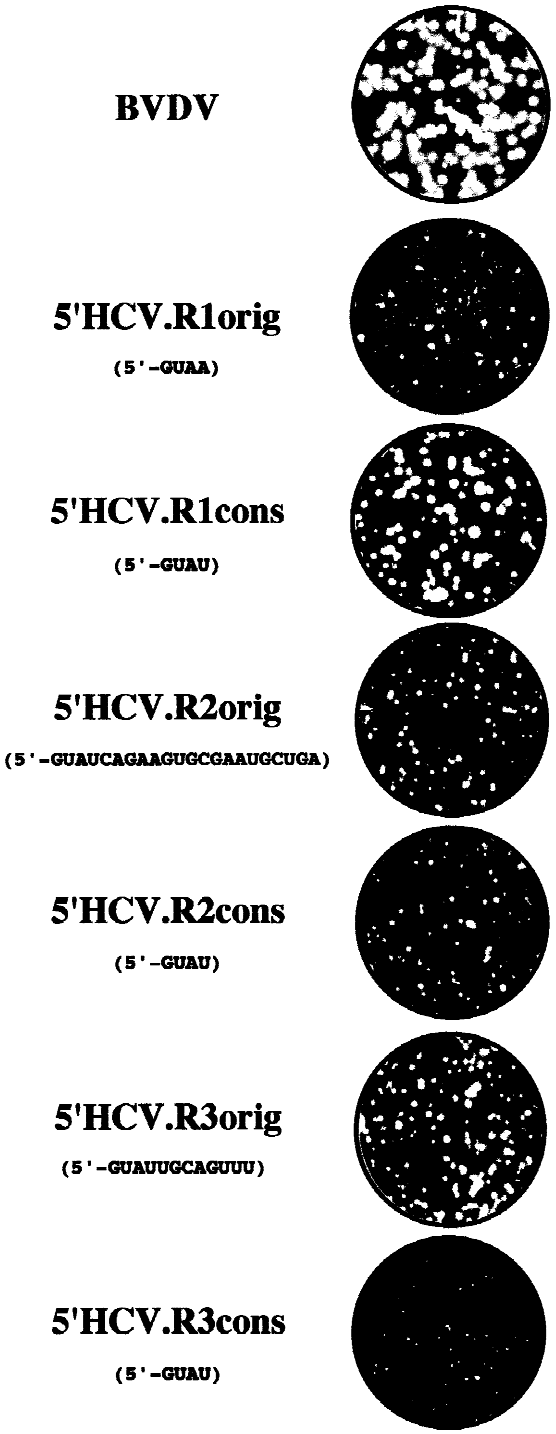

	Translation efficiency (% of BVDV)	Infectivity (PFU/μg of RNA)	Virus titer (PFU/ml)	
			24h	48h
BVDV	100	4×10^6	7×10^7	1×10^8
5'HCV.R1orig (5'-GUAA)	45	4×10^5	2×10^3	2×10^5
5'HCV.R1cons (5'-GUAU)	29	3×10^6	4×10^7	5×10^7
5'HCV.R2orig (5'-GUAUCAGAAGUGCGAAUGCUGA)	17	2×10^6	7×10^6	5×10^7
5'HCV.R2cons (5'-GUAU)	35	3×10^6	2×10^7	4×10^7
5'HCV.R3orig (5'-GUAUUGCAGUUU)	33	3×10^6	4×10^7	5×10^7
5'HCV.R3cons (5'-GUAU)	30	3×10^6	1×10^7	6×10^7

FIGURE 6. (*Legend on facing page.*)

the phenotype of chimeras that lack B1′ and B1 in vivo to determine if they are attenuated and might serve as useful BVDV vaccines. In this vein, several studies with flaviviruses have demonstrated that alterations in 5′ NTR or 3′ NTR elements can lead to attenuation in vivo (Cahour et al., 1995; Men et al., 1996; Mandl et al., 1998). BVDV chimeras that utilize the HCV or EMCV IRES may also prove to be attenuated simply due to the presence of the heterologous IRES. For poliovirus, it has been shown that differences in IRES efficiency in different host-cell environments can modulate host range and virulence (Shiroki et al., 1997).

BVDV–HCV chimeras that are dependent on a functional HCV IRES may have another practical application. It may be possible to use these chimeras to screen for anti-HCV therapeutics that target the HCV IRES. Other researchers have shown antisense oligonucleotide-mediated inhibition of HCV gene expression in hepatocytes by targeting the oligonucleotides to the HCV IRES (Hanecak et al., 1996). It will be of interest to measure the efficacy of antisense oligonucleotides or ribozymes (Lieber et al., 1996) against replicating virus, and these chimeras are more useful than HCV for this purpose since they are able to replicate efficiently in cell culture. We consider BVDV to be a reasonable model of HCV replication not only because of homology and conserved motifs within the 5′ NTR but also because of similarities in overall genetic organization (Rice, 1996) and polyprotein processing strategy (Tautz et al., 1997; Xu et al., 1997). It will be interesting to see if the approach used here can be extended to produce viable BVDV–HCV chimeras dependent upon other HCV functions.

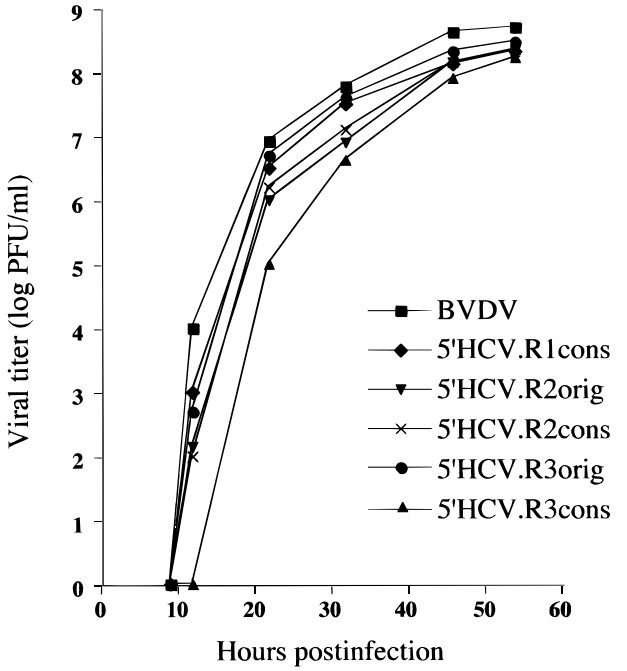

FIGURE 7. Single step growth curve. MDBK cells were seeded on 35-mm dishes (5×10^5 cells/dish) 4 h prior to infection. Infections were performed with an mutiplicity of infection of 1 PFU/cell for 1 h at 5 °C with continuous shaking. The cells were then washed six times with phosphate buffered saline, and 1 ml of D-MEM supplemented with 10% horse serum was added. The cells were then incubated at 37 °C, and media were harvested and replaced at 3, 6, 9, 12, 22, 32, 46, and 54 h postincubation. Released virus titers were measured by performing plaque assays on MDBK cells. The plot shows cumulative viral titers. The detection limit of the plaque assay (shown in the graph as "0" values) was 50 PFU/ml.

MATERIALS AND METHODS

Plasmid Constructs

pACNR/BVDV NADL was previously described (Mendez et al., 1998). pBVDV is a derivative of pACNR/BVDV NADL which contains a G→T transversion at nt 14994 that creates an *Xba* I site upstream of the T7 promoter (T. Myers & C.M. Rice, unpubl.). To facilitate construction of the chimeras, subclones were created. First, two fragments were isolated by PCR amplification of p90/HCVFLlongpU (Kolykhalov et al., 1997) with primers #498 (5′-TGTACATGGCACGTGCCAGCCCCC) and #499 (5′-GATCAACTCCATGGTGCACGGTCT) and pBVDV with primers #481 (5′-AGACCGTGCACCATGGAGTTGATC) and #482 (5′-CGTTTCACACATGGATCCCTCCTC). These two fragments were digested with *Apa*L I and ligated to produce a fragment containing a fusion of the HCV 5′ NTR to the BVDV ORF. This fragment was digested with *Sac* I and ligated into pGEM3Zf(−) which had been digested with *Sma I* and *Sac* I to produce the subclone pGEM498-SacI. Next, a fragment containing the BVDV 5′ NTR was synthesized by PCR amplification of pBVDV with primers #183 (5′-TTTTCTAGATAATACGACTCACTATAGTATACGAGAATTAGAAAAGGCACTCG) and #480 (5′-GGGGGCTGGCACGTGCCATGTACA). This fragment was digested with *Xba* I and *Bsr*G I and ligated into pGEM498-SacI digested with the same two enzymes, to create the plasmid pGEMXbaI-SacI. pGEMXbaI-SacI contains a tandem fusion of the BVDV 5′ NTR, the HCV 5′ NTR, and the 5′ portion of the BVDV N^{pro} gene. pBVDV + HCV was created by digesting pGEMXbaI-SacI with *Xba* I and *Sac* I and ligating the fragment into pBVDV digested with the same two enzymes, and as such

FIGURE 6. Construction of derivatives of 5′HCV designed to contain 5′ termini corresponding to the sequence detected within the three analyzed pseudorevertants. **A**: 5′ terminal sequence of the 5′HCV derivatives. The suffix (orig) designates a derivative containing the original 5′ terminal sequence of the pseudorevertant. The suffix (cons) designates a derivative containing the consensus tetranucleotide sequence 5′-GUAU at the same position. Novel sequences are shown in bold upper case type. **B**: Plaque phenotypes, reticulocyte translation efficiencies relative to parental BVDV, specific infectivities in MDBK cells, and titers at 24 and 48 h posttransfection are indicated.

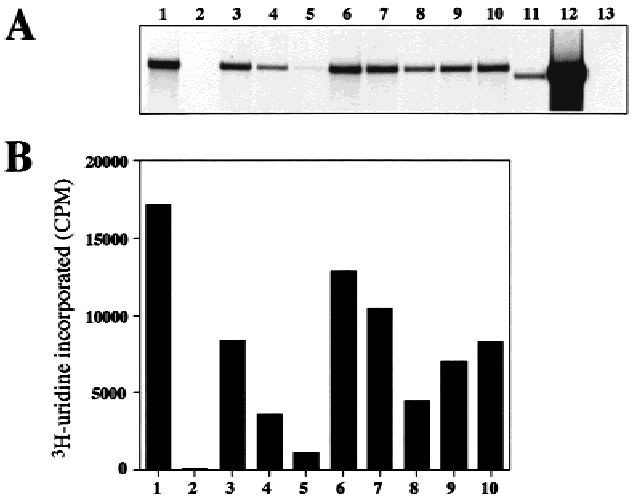

FIGURE 8. Replication of BVDV RNA or chimeric derivatives in transfected MDBK cells. Equal numbers of MDBK cells ($\sim 8 \times 10^6$) were electroporated with 5 μg of each in vitro synthesized RNA. MDBK cells were also transfected with infectious yellow fever 17D (Rice et al., 1989) and Sindbis (Rice et al., 1987) RNAs to provide molecular mass markers. One fifth of the transfected cells were seeded on 35-mm dishes and incubated in D-MEM supplemented with 10% horse serum for 6 h at 37 °C. The media were then replaced with 1 ml of fresh media containing 2 μg/ml of actinomycin D and 40 μCi/ml of ^{3}H-uridine. Incubations were continued for 10 h at 37 °C. RNAs were isolated as described in Materials and Methods, and one quarter of the samples was denatured in glyoxal and loaded on an agarose gel. **A**: Autoradiograph of the dried gel. Only the portion of the gel containing the genomic RNAs is shown. **B**: Amount of radioactivity contained within the displayed fragments as determined by scintillation counting. BVDV, lane 1; 5′HCV, lane 2; BVDV+HCVdelB2B3, lane 3; BVDV+HCVdelB2B3H1, lane 4; 5′HCV.R1orig, lane 5; 5′HCV.R1cons, lane 6; 5′HCV.R3orig, lane 7; 5′HCV.R3cons, lane 8; 5′HCV.R2orig, lane 9; 5′HCV.R2cons, lane 10; yellow fever 17D, lane 11; Sindbis, lane 12; nontransfected MDBK cells, lane 13. The experiments shown is one of two repetitions which yielded similar results.

pBVDV+HCV contains the T7 promoter, followed by the entire 385-nt 5′ NTR of BVDV, a GT dinucleotide (nt 386–387), the entire 341-nt 5′ NTR of HCV (nt 388–728), and the sequence of the BVDV NADL strain including the ORF and 3′ NTR. Derivatives of pBVDV+HCV containing deletions within the BVDV 5′ NTR and/or the HCV 5′ NTR were created in the subclone pGEMXbaI-SacI, as described below, prior to ligation into *Xba* I- and *Sac* I-digested pBVDV. For making deletions, restriction sites with noncompatible protruding ends were treated with the Klenow fragment of DNA polymerase I prior to ligation. For creation of pBVDV+HCVdelB3 (deletion of nt 174–374, inclusive), pGEMXbaI-SacI was digested with *Afl* II and *Bsr*G I. For pBVDV+HCVdelB2B3 (deletion of nt 67–374), pGEMXbaI-SacI was digested with *Avr* II and *Bsr*G I. For pBVDV+HCVdelB1B2B3 (deletion of nt 33–374), pGEMXbaI-SacI was digested with *Sna*B I and *Bsr*G I. For pBVDV+HCVdelB2B3H1 (deletion of nt 67–396), pGEMXbaI-SacI was digested with *Avr* II and *Xcm* I. For pBVDV+HCVdelB2B3H1H2 (deletion of nt 67–513), pGEMXbaI-SacI was digested with *Avr* II and *Bsg* I. For pBVDV+HCVdelB2B3H3 (deletion of nt 67–374, 518–704), subclone pGEMXbaI-SacIdelB2B3 was digested with *Sma* I. p5′HCV was created by digesting p90/HCVFLlongpU with *Xba* I and *Nru* I and ligating the fragment into pBVDV+HCV digested with the same two enzymes.

The EMCV plasmid, pEC$_9$, was provided by Ann Palmenberg and is described elsewhere (Hahn & Palmenberg, 1995). p5′EMCV contains the entire 710 nt of the 5′ NTR of EMCV, followed by the open reading frame of BVDV and the 3′ NTR. One extra G residue was added between the T7 promoter and the first nucleotide of the EMCV 5′ NTR to facilitate efficient in vitro transcription. Convenient restriction sites within the BVDV 5′ NTR or the EMCV 5′ NTR were used to create additional chimeras. Sites with noncompatible protruding ends were treated with the Klenow fragment of DNA polymerase I prior to ligation. For example, the plasmid pBVDV+EMCVdelA contains nt 1–378 of BVDV 5′ NTR fused with nt 45–710 of EMCV (the *Bsr*G I site of BVDV ligated to the *Eco*R V site of EMCV). pBVDV+EMCVdelB3A contains nt 1–173 of BVDV fused with nt 45–710 of EMCV (the *Afl* II site of BVDV ligated to the *Eco*R V site of EMCV). pBVDV+EMCVdelB2B3A contains nt 1–66 of BVDV fused with nt 45–710 of EMCV (the *Avr* II site of BVDV ligated to the *Eco*R V site of EMCV). pBVDV+EMCVdelB3ABC contains nt 1–173 of BVDV fused with nt 161–710 of EMCV (the *Afl* II site of BVDV ligated to the *Psp*1406 site of EMCV). pBVDV+EMCVdelB2B3ABC nt 1–66 of BVDV fused with nt 161–710 of EMCV (the *Avr* II site of BVDV ligated to the *Psp*1406 site of EMCV). pBVDV+EMCVdelB3A-H contains nt 1–101 of BVDV fused with nt 289–710 of EMCV (the *Nhe I* site of BVDV ligated to the *Avr* II site of EMCV). pBVDV+EMCVdelB2B3A-H contains nt 1–62 of BVDV fused with nt 289–710 of EMCV (the *Avr* II site of BVDV ligated to the *Avr* II site of EMCV). The schematics of the chimeric 5′ NTRs are presented in Figures 2 and 4.

All other heterologous 5′ NTRs used in the study were generated by PCR using an oligonucleotide complementary to nt 256–272 of the HCV 5′ NTR and primers containing the sequence of the *Xba* I restriction site followed by the T7 promoter, the heterologous sequences found in sequenced pseudorevertants, or sequences corresponding to different regions of the HCV 5′ NTR. All the fragments were subcloned into the plasmid, pRS2 (a derivative of pUC19), sequenced, and recloned into the p5′HCV plasmid by replacing the fragment between the *Xba* I site located upstream of the T7 promoter and the *Nhe* I site (nt 249–254) in the 5′ NTR of HCV.

Cell cultures

MDBK cells were obtained from M. Collett (ViroPharma, Incorporated) and BT cells were obtained from the American Type Culture Collection (Rockville, Maryland). Cells were grown in Dulbecco's modified Eagle medium (D-MEM) supplemented with 10% horse serum and sodium pyruvate.

Transcriptions and transfections

All the designed plasmids, including pBVDV and the chimeric derivatives, were digested to completion with *Sda* I (*Sse*8387I), purified by phenol extraction, precipitated by ethanol, and dissolved in water. The transcription reactions were performed using the T7 Megascript kit (AMBION) using the conditions recommended by the manufacturer. Reactions were

incubated at 37 °C for 1 h, and ^{3}H-UTP was added to the reaction to quantify the RNA synthesis. The quality of the synthesized RNAs was checked by agarose gel electrophoresis, and samples containing 50–60% of full-length RNA were used for electroporations and in vitro translations. The reaction mixtures were aliquoted and stored at −70 °C prior to electroporation or in vitro translations.

Transfection was performed by electroporation of MDBK cells using previously described conditions (Mendez et al., 1998). Two micrograms of in vitro synthesized RNA, corresponding to approximately 1 μg of the full-length transcript, were used per electroporation. In standard experiments, tenfold dilutions of electroporated cells were seeded in 6-well tissue culture plates containing 5×10^5 naive MDBK cells per well. After 1 h of incubation at 37 °C in an 5% CO_2 incubator, cells were overlaid with 3 ml of 0.6% LE Sea Kem agarose (FMC Bioproducts) containing minimal essential medium supplemented with 5% horse serum. Plaques were stained with crystal violet after 3 days incubation at 37 °C. The rest of the transfected cells was seeded into 100-mm dishes and incubated for approximately 48 h or until cytopathic effect was observed in virtually all cells. Samples of the media were taken at 24 and 48 h, and virus titers were determined as described above and previously (Mendez et al., 1998).

Analysis of the 5′ ends of viral genomes

Sequencing of the 5′ ends of selected variants of BVDV was performed on plaque-purified viruses. Plaques were typically isolated from the agarose overlay without staining with neutral red. Virus was eluted in 1 ml of D-MEM/10% horse serum for several hours and was used to infect 5×10^5 MDBK cells in 35-mm dishes. After 1 h of virus adsorption at 37 °C, an additional 1 ml of D-MEM/10% horse serum was added to the dishes, and incubation was continued for 36–48 h until cytopathic effect was observed in virtually all cells.

Fifty microliters of harvested viral stocks were clarified by low speed centrifugation, and viral RNAs were isolated by TRIzol reagent (Gibco-BRL) using the protocol recommended by the manufacturer. Sequencing of the 5′ termini was performed using an oligonucleotide/cDNA-ligation strategy described elsewhere (Troutt et al., 1992). The primer S1 (5′-GTCGTTTCACACATGGATCC), complementary to nt 710–729 of the BVDV genome, was used for cDNA synthesis. A phosphorylated oligonucleotide tag (5′-GACTGTTGTGGCC TGCAGGGCCGAATT) with an amino group on the 3′ terminus was ligated to the first strand cDNA (Troutt et al., 1992). One tenth of this reaction mixture was used for PCR amplification. The primers for PCR amplification were as follows: primer A (5′-GCCCTGCAGGCCACAACAGTC), complementary to the tag; primer B (5′-TCAGGCAGTACCACAA) complementary to nt 281–296 of the HCV 5′ NTR; and primer C (5′-GGAATGCTCGTCAAGAAGACAG), complementary to nt 268–289 of the EMCV 5′ NTR. The primer pairs of A + B or A + C were used for analysis of the pseudorevertants of 5′HCV and BVDV + HCVdelB1B2B3 or 5′EMCV, respectively. For the 5′HCV pseudorevertants, one tenth of the ligation mixture was used for an additional PCR reaction. This fragment was synthesized using primer S1, described above, and a primer corresponding to nt 147–175 of the HCV genome. Fragments were purified by agarose gel electrophoresis and cloned into the plasmid pRS2. Multiple independent clones were sequenced by the standard dideoxy-mediated chain termination method using the Sequenase version 2.0 DNA Sequencing Kit (USB).

Cell-free translation

Cell-free translation reactions were performed in reticulocyte extracts (Promega) using conditions recommended by the manufacturer. Usually 0.1–1 μg of the same in vitro synthesized RNAs used in transfection experiments were used in 25 μl translation reactions. After 45 min of incubation at 30 °C, 2 μl were dissolved in 10 μl of sample buffer, and those samples were analyzed by sodium dodecyl sulfate PAGE. Labeled proteins were visualized by autoradiography of the dried gel. The efficiency of translation was measured using phosphorimager analysis (Molecular Dynamics) by comparing the radioactivity in the band corresponding to the N^{pro} protein. In preliminary experiments, an eightfold increase in incorporation was observed for translation of 4 μg versus 0.4 μg BVDV transcript RNA. Quantitative data were obtained from reactions using subsaturating (0.4 μg) amounts of BVDV or BVDV chimera transcript RNAs.

Analysis of virus specific RNAs

The protocols used for radioactive labeling of virus-specific RNAs are described in the appropriate figure legends. RNAs were isolated from the cells by using TRIzol reagent as recommended by the manufacturer (Gibco-BRL). After denaturation with glyoxal in dimethylsulfoxide, cellular RNAs were analyzed by electrophoresis in a 1% agarose gel containing a 10 mM phosphate buffer. Pieces of the dried gel containing the appropriate RNA bands were excised, and their radioactivity measured by liquid scintillation counting.

ACKNOWLEDGMENTS

We thank Tina Myers for help in creating the plasmid, pBVDV. We also thank Carol Read and Rebecca Moran for expert technical assistance. We are also grateful to John Majors, Tina Myers, Ann Palmenberg, and Karen Reed for critical reading of the manuscript.

Received June 16, 1998; returned for revision July 30, 1998; revised manuscript received August 4, 1998

REFERENCES

Ball LA. 1994. Replication of the genomic RNA of a positive-strand RNA animal virus from negative-sense transcripts. *Proc Natl Acad Sci USA 91*:12443–12447.

Becher P, Orlich M, Thiel H-J. 1998. Complete genomic sequence of border disease virus, a pestivirus from sheep. *J Virol 72*:5165–5173.

Brown EA, Zhang H, Ping LH, Lemon SM. 1992. Secondary structure of the 5′ nontranslated regions of hepatitis C virus and pestivirus genomic RNAs. *Nucleic Acids Res 20*:5041–5045.

Bukh J, Purcell RH, Miller RH. 1992. Sequence analysis of the 5′ noncoding region of hepatitis C virus. *Proc Natl Acad Sci USA 89*:4942–4946.

Cahour A, Pletnev A, Vazielle FM, Rosen L, Lai CJ. 1995. Growth-restricted dengue virus mutants containing deletions in the 5′ noncoding region of the RNA genome. *Virology 207*:68–76.

Deng R, Brock KV. 1993. 5′ and 3′ untranslated regions of pestivirus genome: Primary and secondary structure analyses. *Nucleic Acids Res 21*:1949–1957.

Duke GM, Hoffman MA, Palmenberg AC. 1992. Sequence and structural elements that contribute to efficient encephalomyocarditis virus RNA translation. *J Virol 66*:1602–1609.

Duke GM, Osorio JE, Palmenberg AC. 1990. Attenuation of Mengo virus through genetic engineering of the 5′ noncoding poly(C) tract. *Nature 343*:474–476.

Guan H, Song C, Simon AE. 1997. RNA promoters located on (−)-strands of a subviral RNA associated with turnip crinkle virus. *RNA 3*:1401–1412.

Hahn H, Palmenberg AC. 1995. Encephalomyocarditis viruses with short poly(C) tracts are more virulent than their mengovirus counterparts. *J Virol 69*:2697–2699.

Hanecak R, Brown DV, Fox MC, Azad RF, Furusako S, Nozaki C, Ford C, Sasmor H, Anderson KP. 1996. Antisense oligonucleotide inhibition of hepatitis C virus gene expression in transformed hepatocytes. *J Virol 70*:5203–5212.

Hoffman MA, Palmenberg AC. 1996. Revertant analysis of J-K mutations in the encephalomyocarditis virus internal ribosomal entry site detects an altered leader protein. *J Virol 70*:6425–6430.

Honda M, Brown EA, Lemon SM. 1996a. Stability of a stem-loop involving the initiator AUG controls the efficiency of internal initiation of translation on hepatitis C virus RNA. *RNA 2*:955–968.

Honda M, Ping LH, Rijnbrand RC, Amphlett E, Clarke B, Rowlands D, Lemon SM. 1996b. Structural requirements for initiation of translation by internal ribosome entry within genome-length hepatitis C virus RNA. *Virology 222*:31–42.

Houghton M. 1996. Hepatitis C viruses. In: Fields BN, Knipe DM, Howley PM, eds. *Fields virology*. Philadelphia: Lippincott-Raven Publishers. pp 1035–1058.

Huang HV. 1997. Evolution of the alphavirus promoter and the *cis*-acting sequences of RNA viruses. In: Saluzzo J-F, Dodet B, eds. *Factors in the emergence of arbovirus diseases*. Paris: Elsevier Press. pp 65–79.

Jang SK, Kräusslich H-G, Nicklin MJ, Duke GM, Palmenberg AC, Wimmer E. 1988. A segment of the 5′ nontranslated region of encephalomyocarditis virus RNA directs internal entry of ribosomes during in vitro translation. *J Virol 62*:2636–2643.

Jang SK, Wimmer E. 1990. Cap-independent translation of encephalomyocarditis virus RNA: Structural elements of the internal ribosomal entry site and involvement of a cellular 57-kD RNA-binding protein. *Genes & Dev 4*:1560–1572.

Kamoshita N, Tsukiyama KK, Kohara M, Nomoto A. 1997. Genetic analysis of internal ribosomal entry site on hepatitis C virus RNA: Implication for involvement of the highly ordered structure and cell type-specific transacting factors. *Virology 233*:9–18.

Kirkegaard K, Baltimore D. 1986. The mechanism of RNA recombination in poliovirus. *Cell 47*:433–443.

Kolykhalov AA, Agapov EV, Blight KJ, Mihalik K, Feinstone SM, Rice CM. 1997. Transmission of hepatitis C by intrahepatic inoculation with transcribed RNA. *Science 277*:570–574.

Kolykhalov AA, Feinstone SM, Rice CM. 1996. Identification of a highly conserved sequence element at the 3′ terminus of hepatitis C virus genome RNA. *J Virol 70*:3363–3371.

Le SY, Siddiqui A, Maizel JV Jr. 1996. A common structural core in the internal ribosome entry sites of picornavirus, hepatitis C virus, and pestivirus. *Virus Genes 12*:135–147.

Lemon SH, Honda M. 1997. Internal ribosome entry sites within the RNA genomes of hepatitis C virus and other flaviviruses. *Semin Virol 8*:274–288.

Lieber A, He C-Y, Polyak SJ, Gretch DR, Barr D, Kay MA. 1996. Elimination of hepatitis C virus RNA in infected human hepatocytes by adenovirus-mediated expression of ribozymes. *J Virol 70*:8782–8791.

Lima WF, Brown DV, Fox M, Hanecak R, Bruice TW. 1997. Combinatorial screening and rational optimization for hybridization to folded hepatitis C virus RNA of oligonucleotides with biological antisense activity. *J Biol Chem 272*:626–638.

Lu HH, Wimmer E. 1996. Poliovirus chimeras replicating under the translational control of genetic elements of hepatitis C virus reveal unusual properties of the internal ribosomal entry site of hepatitis C virus. *Proc Natl Acad Sci USA 93*:1412–1417.

Mandl CW, Holzmann H, Meixner T, Rauxcher S, Stadler PF, Allison SL, Heinz FX. 1998. Spontaneous and engineered deletions in the 3′ noncoding region of tick-borne encephalitis virus: Construction of highly attenuated mutants of a flavivirus. *J Virol 72*:2132–2140.

Martin LR, Palmenberg AC. 1996. Tandem mengovirus 5′ pseudoknots are linked to viral RNA synthesis, not poly(C)-mediated virulence. *J Virol 70*:8182–8186.

Men R, Bray B, Clark D, Chanock RM, Lai CJ. 1996. Dengue type 4 virus mutants containing deletion in the 3′ noncoding region of the RNA genome: Analysis of growth restriction in cell culture and altered viremia pattern and immunogenicity in rhesus monkeys. *J Virol 70*:3930–3937.

Mendez E, Ruggli N, Collett MS, Rice CM. 1998. Infectious bovine viral diarrhea virus (Strain NADL) RNA from stable cDNA clones: A cellular insert determines NS3 production and viral cytopathogenicity. *J Virol 72*:4737–4745.

Meyers G, Thiel H-J. 1996. Molecular characterization of pestiviruses. *Adv Virus Res 47*:53–118.

Monath TP, Heinz FX. 1996. Flaviviruses. In: Fields BN, Knipe DM, Howley PM, eds. *Fields virology*. New York: Raven Press. pp 961–1034.

Palmenberg AC, Sgro J-Y. 1997. Topological organization of picornaviral genomes: Statistical prediction of RNA structural signals. *Semin Virol 8*:231–241.

Poole TL, Wang C, Popp RA, Potgieter LN, Siddiqui A, Collett MS. 1995. Pestivirus translation initiation occurs by internal ribosome entry. *Virology 206*:750–754.

Pugachev KV, Frey TK. 1998. Effects of defined muations in the 5′ nontranslated region of rubella virus genome RNA on virus viability and macromolecule synthesis. *J Virol 72*:641–650.

Reynolds JE, Kaminski A, Carroll AR, Clarke BE, Rowlands DJ, Jackson RJ. 1996. Internal initiation of translation of hepatitis C virus RNA: The ribosome entry site is at the authentic initiation codon. *RNA 2*:867–878.

Reynolds JE, Kaminski A, Kettinen HJ, Grace K, Clarke BE, Carroll AR, Rowlands DJ, Jackson RJ. 1995. Unique features of internal initiation of hepatitis C virus RNA translation. *EMBO J 14*:6010–6020.

Rice CM. 1996. *Flaviviridae*: The viruses and their replication. In: Fields BN, Knipe DM, Howley PM, eds. *Fields virology*. Philadelphia: Lippincott-Raven Publishers. pp 931–960.

Rice CM, Grakoui A, Galler R, Chambers TJ. 1989. Transcription of infectious yellow fever virus RNA from full-length cDNA templates produced by in vitro ligation. *New Biol 1*:285–296.

Rice CM, Levis R, Strauss JH, Huang HV. 1987. Production of infectious RNA transcripts from Sindbis virus cDNA clones: Mapping of lethal mutations, rescue of a temperature-sensitive marker, and in vitro mutagenesis to generate defined mutants. *J Virol 61*:3809–3819.

Rijnbrand R, Bredenbeek PJ, van der Straaten T, Whetter L, Inchauspe G, Lemon S, Spaan W. 1995. Almost the entire 5′ non-translated region of hepatitis C virus is required for cap-independent translation. *FEBS Lett 365*:115–119.

Rijnbrand R, van der Straaten T, van Rijn PA, Spaan WJ, Bredenbeek PJ. 1997. Internal entry of ribosomes is directed by the 5′ noncoding region of classical swine fever virus and is dependent on the presence of an RNA pseudoknot upstream of the initiation codon. *J Virol 71*:451–457.

Rijnbrand RC, Abbink TE, Haasnoot PC, Spaan WJ, Bredenbeek PJ. 1996. The influence of AUG codons in the hepatitis C virus 5′ nontranslated region on translation and mapping of the translation initiation window. *Virology 226*:47–56.

Ruggli N, Rice CM. 1998. Functional cDNA clones of the *Flaviviridae*: strategies and applications. *Adv Virus Res.* In press.

Ruggli N, Tratschin JD, Mittelholzer C, Hofmann MA. 1996. Nucleotide sequence of classical swine fever virus strain Alfort/187 and transcription of infectious RNA from stably cloned full-length cDNA. *J Virol 70*:3478–3487.

Shiroki K, Ishii T, Aoki T, Ota Y, Yang WX, Komatsu T, Ami Y, Arita M, Abe S, Hashizume S, Nomoto A. 1997. Host range phenotype induced by mutations in the internal ribosomal entry site of poliovirus RNA. *J Virol 71*:1–8.

Tanaka T, Kato N, Cho M-J, Sugiyama K, Shimotohno K. 1996. Structure of the 3′ terminus of the hepatitis C virus genome. *J Virol 70*:3307–3312.

Tautz N, Elbers K, Stoll D, Meyers G, Thiel H-J. 1997. Serine protease of pestiviruses: Determination of cleavage sites. *J Virol 71*:5415–5422.

Thiel H-J, Plagemann PGW, Moennig V. 1996. Pestiviruses. In: Fields BN, Knipe DM, Howley PM, eds. *Fields virology*. New York: Raven Press. pp 1059–1073.

Troutt AB, McHeyzer-Williams MG, Pulendran B, Nossal GJ. 1992. Ligation-anchored PCR: A simple amplification technique with single-sided specificity. *Proc Natl Acad Sci USA 89*:9823–9825.

Tsukiyama-Kohara K, Iizuka N, Kohara M, Nomoto A. 1992. Internal ribosome entry site within hepatitis C virus RNA. *J Virol 66*:1476–1483.

Urabe M, Hasumi Y, Ogasawara Y, Matsushita T, Kamoshita N, Nomoto A, Colosi P, Kurtzman GJ, Tobita K, Ozawa K. 1997. A novel dicistron AAV vector using a short IRES segment derived from hepatitis C virus genome. *Gene 200*:157–162.

Wang C, Le SY, Ali N, Siddiqui A. 1995. An RNA pseudoknot is an essential structural element of the internal ribosome entry site located within the hepatitis C virus 5′ noncoding region. *RNA 1*:526–537.

Wang C, Sarnow P, Siddiqui A. 1993. Translation of human hepatitis C virus RNA in cultured cells is mediated by an internal ribosome-binding mechanism. *J Virol 67*:3338–44.

Wang C, Sarnow P, Siddiqui A. 1994. A conserved helical element is essential for internal initiation of translation of hepatitis C virus RNA. *J Virol 68*:7301–7307.

Wang C, Siddiqui A. 1995. Structure and function of the hepatitis C virus internal ribosome entry site. *Curr Top Microbiol Immunol 203*:99–115.

Xu J, Mendez E, Caron PR, Lin C, Murcko MA, Collett MS, Rice CM. 1997. Bovine viral diarrhea virus NS3 serine proteinase: Polyprotein cleavage sites, cofactor requirements, and molecular model of an enzyme essential for pestivirus replication. *J Virol 71*:5312–5322.